Icons for the visualization of Tensor Fields

Attilio De Liberato and Laura Moltedo
Istituto per le Applicazioni del Calcolo -IAC- C. N. R.
Viale del Policlinico 137 00161 Rome, Italy.
email: moltedo@cnriac.iac.rm.cnr.it

Abstract

Multidimensional data coming from numerical simulations represent, usually, tensor fields. This paper deals with glyph icons we implemented for discrete visualization of second order tensor fields, in order to extend the mapping operations of MUDI3 system we have developed at IAC. Iconic representations of tensor fields we used to study a molecular dynamics problem are discussed too.
Keywords:tensor fields visualization, glyphs, icons, stress tensor.

1 Introduction

Numerical simulations produce, nowadays, a big amount of data, whose analysis becomes easier if visual representations can be provided to the scientists. Very often it deals with large multivariate 3-D data sets. The visualization describes numerical data as "easily to understand" images that allow a rapid and global view of the simulation results. The development of 3-D visualization techniques to derive as much information as possible from the image is one of the main research areas in the scientific visualization, strictly aimed to enhance the quality of the user-image interaction.
The icons can be a good communication tool in such an area, since they are symbols or pictorial representations which are similar with physical objects, actions or functions. Infact, in the context of multivariate data representation, the icons can encode the dependent (spatial) variables as their position and the values of field variables as geometric characteristics such as lenghts, angles, or shapes, or as visible attributes as color, opacity [1].
In this paper we deal with the activity we made in order to represent multidimensional data by means of icons, considering the visualization of second order tensor fields defined over three-dimensional domains.
In section 2 we focus on the problem of visualizing real and simmetric tensor field by introducing the concept of tensor glyph [3] and we describe the implemented

procedure.
In order to use *Tensor Glyph* procedure in an interactive environment it was inserted in MUDI3 [4], a system oriented to the interactive visualization of multidimensional data. In such a way we can use MUDI3 transformations and rendering operations for tensor fields visualization enhancement.
The last section includes the description of an application problem, coming from Molecular Dynamics area, whose data have been studied in cooperation with researchers of the Physics Department of the University of Rome. The enclosed images demonstrate that the glyph representation gives us information more complete than the ones provided by the other techniques. It allows also something like a monitoring of computation method, as we point out in section 3.

2 Tensor fields visualization techniques

This section includes a brief recall of stress tensor, principal stresses, planes and directions. Main parameters and methods for the visualization of second order tensor fields are then described. In conclusion we describe the tensor glyph technique we implemented.

2.1 Some definitions

In order to identify which values are to be computed for representing a second order tensor field, we have to clarify the meaning of stress tensor, principal stresses, planes and directions.
A *second-order tensor* is a quantity uniquely specified by 3^2 real numbers which transforms under changes of the coordinate system according to the law [5]:

$$A'_{ik} = \alpha_{i'l}\alpha_{k'm}A_{lm}, \tag{1}$$

where A_{lm}, A'_{ik} are components of the tensor in the old and new coordinate system K and K', respectively, and $\alpha_{i'l}$ is the cosine of the angle between the ith axis of K' and the lth of K.
A great diversity in notation for stress components exists in literature. The most widely used notation is, in reference to a system of rectangular Cartesian coordinates x, y, z:

$$\|T\| = \begin{pmatrix} \sigma_x & \tau_{xy} & \tau_{xz} \\ \tau_{yx} & \sigma_y & \tau_{yz} \\ \tau_{zx} & \tau_{zy} & \sigma_z \end{pmatrix}, \tag{2}$$

where σ_x, σ_y, σ_z are called *normal stresses* and τ_{xy}, τ_{yx}, τ_{yz}, τ_{zy}, τ_{zx}, τ_{xz} the *shear stresses.*
If the nine cartesian components σ_x, σ_y, σ_z, τ_{xy}, τ_{yx}, τ_{yz}, τ_{zy}, τ_{zx}, τ_{xz} are known,

we can write the stress vector acting on any surface with unit outer normal $\mathbf{n}$ of components $\cos(\mathbf{n}, x)$, $\cos(\mathbf{n}, y)$, $\cos(\mathbf{n}, z)$.
If $\mathbf{P}_n$ is the *stress tensor*, its components p_{nx}, p_{ny}, p_{nz} are given by the Eqs. [6]:

$$\begin{aligned} p_{nx} &= \sigma_x \cos(\mathbf{n}, x) + \tau_{yx} \cos(\mathbf{n}, y) + \tau_{zx} \cos(\mathbf{n}, z) \\ p_{ny} &= \tau_{xy} \cos(\mathbf{n}, x) + \sigma_y \cos(\mathbf{n}, y) + \tau_{zy} \cos(\mathbf{n}, z) \\ p_{nz} &= \tau_{xz} \cos(\mathbf{n}, x) + \tau_{yz} \cos(\mathbf{n}, y) + \sigma_z \cos(\mathbf{n}, z). \end{aligned} \tag{3}$$

With every state of stress, in any point, we can associate no more than three distinct normal stresses on planes free from shear stresses. Such stresses are called *principal stresses*; the planes on which they act are the *principal planes*; and the directions of the outer normals to these principal planes are the *principal directions.*
Let $\sigma_1, \sigma_2, \sigma_3$, be the three principal stresses characterizing the state of stress at a point in the body, and for convenience let them be ordered in the manner $\sigma_1 \geq \sigma_2 \geq \sigma_3$. Consider a "local" cartesian coordinate system centered at the point, with its x, y, and z axes parallel to the principal directions corresponding to $\sigma_1, \sigma_2, \sigma_3$, respectively. There is no lost of generality in carrying out the discussion for a coordinate system so oriented, since it can be established that the principal direction can be determined for any given state of stress.
With the above conventions, the cartesian stress components become:

$$\sigma_x = \sigma_1; \quad \sigma_y = \sigma_2; \quad \sigma_z = \sigma_3; \quad \tau_{xy} = \tau_{yz} = \tau_{xy} = 0$$

and the equations (3):

$$p_{nx} = \sigma_1 \cos(n, x); \quad p_{ny} = \sigma_2 \cos(n, y); \quad p_{nz} = \sigma_3 \cos(n, z). \tag{4}$$

2.2 Parameters for the visualization of tensor fields

Second order threedimensional tensors are fundamental values in a wide range of application fields [7]. Stresses and strains referred to solid objects identify tensor fields. In fluidynamics, stresses, viscous stresses, rate of strain and momentum are described as tensor data. In steady-state Navier-Stokes equations describing gasdynamics problems with only one quantity, momentum flux density is a tensor field.
Since a lot of variables can give information concerning a tensor field, we need to accurately individuate, among them, the parameters which are useful for the visualization. As we anticipated in section 2.1, a second order tensor field defined over a threedimensional domain is represented by a 3x3 array of scalar functions (2).
The independent visualization of these nine functions is possible, but it could be not easy to interpret. In our work we considered only real and symmetric tensors, but it can be demonstrated that a wide class of antisymmetric real and complex Hermitian tensor fields can be reduced to a sum of real and symmetric tensors and a

vector field. For example the velocity gradient in a fluid is composed by the sum of rate of strain tensor and the rate of rotation that are, respectively, symmetric and antisymmetric tensor fields.
Now we consider a real symmetric tensor field, that is a law that maps to each point x of the space a tensor, as a 3x3 array $\|T(x)\|$ with the condition that $\tau_{ik} = \tau_{ki}$. $|T(x)|$ has three real eigenvalues $\sigma_1, \sigma_2, \sigma_3$ and three real and orthogonal eigenvectors $e^{(1)}(x)$, $e^{(2)}(x)$, $e^{(3)}(x)$ at every point x in the space. Instead of considering the single scalar components of $\|T(x)\|$, we can take into account the three orthogonal vector fields:

$$v^{(i)}(x) = \sigma^{(i)}(x)e^{(i)}(x).$$

We can conclude that the visualization of a symmetric real tensor field is equivalent to the simultaneous visualization of three orthogonal vector fields, since they include all the information concerning the amplitude (the eigenvalues) and the direction (the eigenvectors) which are represented, in matricial notation, by the components of $\|T(x)\|$.

2.3 Discrete visualization of tensor fields

Direct and indirect methods are used for the visualization of tensor fields [3]. Direct methods provide a symbolic representation of the local magnitude and direction of the vector field. Indirect methods describe the physical effect of the vector field and give only an idea of the its local characteristics. In other words, a direct method corresponds to a discrete visualization, generally realized by means of an iconic symbol, whereas indirect methods allow continuous representations.
Discrete representation methods have been considered in our work.
A technique for a discrete representation of a tensor field is the Lamé Stress Ellipsoid [6]. In fact, if Eqs. (3) are solved for three direction cosines, then, squared and added, the Eq. :

$$\frac{p_{nx}^2}{\sigma_1^2} + \frac{p_{ny}^2}{\sigma_2^2} + \frac{p_{nz}^2}{\sigma_3^2} = 1, \tag{5}$$

is obtained, since the sum of the squares of the direction cosines is equal to unity. This is the equation of an ellipsoid referred to a coordinate system having p_{nx}, p_{ny}, p_{nz} as cartesian axes (principal coordinate system). Considering these stress components synonymous with the coordinates x, y and z of the local coordinate system at the point, the previous equation can be written :

$$\frac{x^2}{\sigma_1^2} + \frac{y^2}{\sigma_2^2} + \frac{z^2}{\sigma_3^2} = 1. \tag{6}$$

The surface is called the stress ellipsoid or the ellipsoid of Lamé. It has the property that the lenght of the radius vector from origin O to a point $P(xyz) = P(p_{nx}, p_{ny}, p_{nz})$ on the ellipsoid surface is equal to the magnitude of the stress acting on the plane through $P(x, y, z)$.

Figure 1: Glyph-icon for the tensor fields representation.

The semiaxes lenght is equal to the magnitudes of the principal stresses at the point, i.e. the minor and the major semiaxis of the ellipsoid represent, respectively, the minor and the major stresses acting on all the planes through the point.
There are degenerate cases of ellipsoid. The ellipsoid becomes an ellipsoid of revolution about the axis parallel to the third stress when two of the principal stresses are equal. It becomes a sphere when all the principal stresses are equal.
The Stress Quadric of Cauchy [8] is another method for representing the equations governing the state of stress at a point. Consider the quadric surface:

$$\sigma_1 x^2 + \sigma_2 y^2 + \sigma_3 z^2 = \pm 1,$$

constructed in the local coordinate system at the point. This surface allows a more complete representation of stress tensor information. However, it is not an intuitive representation. In fact, it takes considerable effort to interpret the directional information, and the quadric surface can be self-occluding.
In this paper we are describing a direct method based on tensor glyph for the visualization of second order tensor field. In [3] a glyph is defined as a geometric icon that represents multi-variate or higher-dimensional information at given positions. Data values are mapped to various physical attributes of the icon as geometry, color, surface, texture. Therefore, we can describe all the information included in the tensor data by means of a glyph visualized in each sampled point. The tensor glyph of the figure 1 derives from the Lamé Stress Ellipsoid. In fact, a modified geometry can be used for the construction of such an icon, in order to indicate directions and magnitudes of the principal stresses. The color is used to encode their signs.
We can summarize the procedure for the construction of the tensor glyph in the following actions. Firtsly, we have to compute direction and sign of the principal stresses in each point (where the stress is known) and to construct a cylindrical shaft having the direction of the major principal stress and the lenght proportional to its magnitude. Minor and major radii of the elliptical disk, that is built around the central portion of shaft, represent, respectively, magnitudes and directions of the minor and the middle principal stresses. It is possible to scale the dimensions of the disk by a factor α, according to the lenght of the shaft. Colors are associated with the shaft and disk surface in order to indicate, as mentioned above, the signs of the principal stresses: blue indicates tension, yellow indicates compression.
The procedure also deals with the degenerate cases, i.e. when some of the stresses vanish. In fact, the elliptical disk is reduced to a segment or the shaft becomes a circle if one of the principal stresses is equal to zero. The elliptical disk becomes a point or a segment and the shaft becomes a circle if two of the principal stresses are equal to zero. The tensor glyph is not visualized if all the principal stresses are equal to zero.

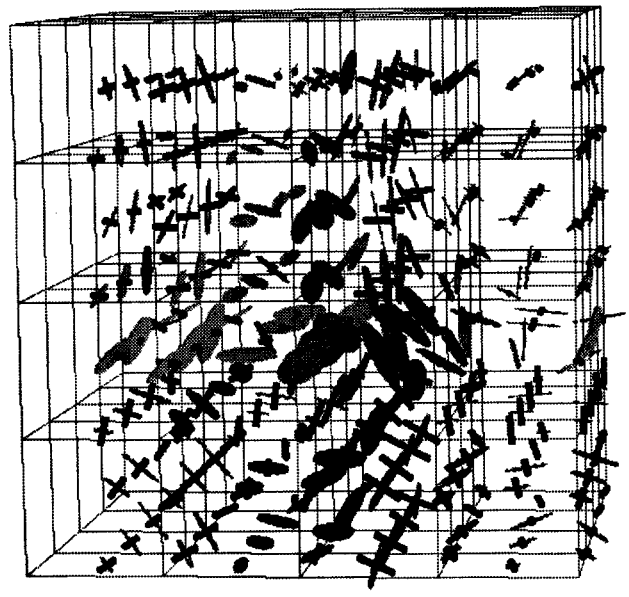

Figure 2: Non simmetric tensor field derived from a computational code with a fixed origin of the coordinates.

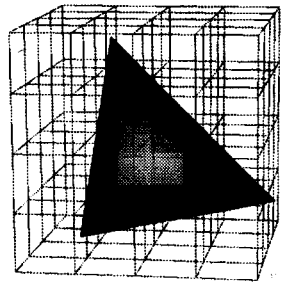

Figure 3: Miller's plane indicates the zone where the stresses rapidly vary.

3 An interactive visualization of tensor fields to study a molecular dynamics problem

In order to use the procedure *Tensor Glyph* in an interactive environment, we inserted it into a system oriented to the multidimensional data interactive visualization, named MUDI3, that has been designed at IAC [4]. The system runs under UNIX workstations and it consists of C programs that use the PEX graphics library [10].
At WSCG'95 [2] we presented the MUDI3 functionalities and some experiments carried out for testing cognitive and perception aspects of its iconic interface.
Here we include the results and the images dealing with an application, aimed to the interactive visualization of second order tensor fields by means of tensor glyphs.
The figures 2,3,4 show the images derived from the visualization of data produced by a computing code of a Molecular Dynamics problem. This code has been used at the Physics Department of the University of Rome "La Sapienza" for studying a

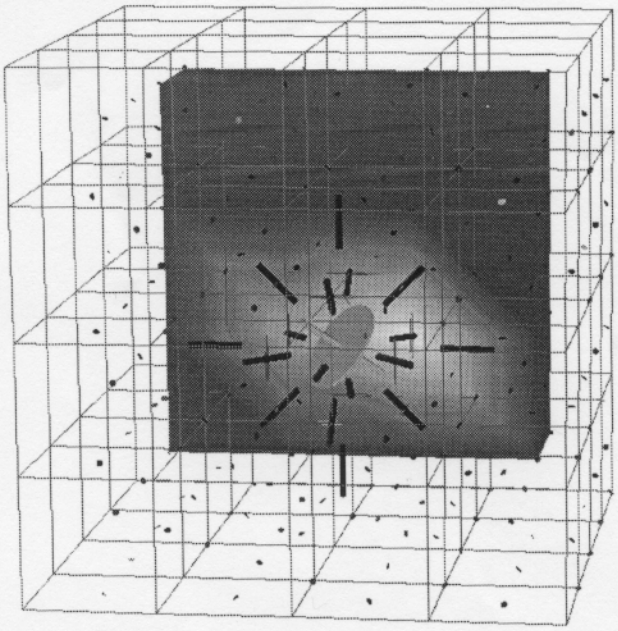

Figure 4: Symmetric tensor and scalar fields derived from a computational code with a new origin of the coordinates at the centre of each microscopic volume.

phenomenon of mixture of hydrogen in palladium. Particularly, the study is focused on the behaviour of a palladium crystal in which some hydrogen atoms are sparsely included. The mycroscopic observation indicates that, in particular termodynamical conditions, outside from the coexistence zone, the hydrogen is concentrated in some points of the crystal without further uniform mixtures. The condensation of the hydrogen in the solid produces a force field in the lattice of the metal. Such forces cause a stress field that becomes a strain field if the solid is allowed to relax.
A relevant and still unsolved question in the physics of hydrogenated metals is the range of the strain field generated by a droplet of hydrogen atoms field in the metallic matrix. This field is regarded as a possible cause for the remarkable condensation capability of hydrogen atoms in the coexistence region of the phase diagram [11]. The computation of the stress tensor field is, in this case, no trivial, because one expects the fields vary significantly over distances of the order of the cell parameter of the lattice. One has thus to define the stress tensor, which is usually thought as a hydrodinamical field, in a microscopic volume entailing few atoms (actually: one atom and its six first neighbours in the face centered cubic (fcc) structure of Palladium). Moreover, as the interaction potential of Palladium has a many-body nature [12, 13], no clear definition is possible of the "forces crossing the surfaces of the volume", as it is usually done in the elasticity theory [14]. The only practical way to compute a stress tensor field is, in this case, to apply the formula:

$$\pi_{\alpha,\beta} = \sum_i r_\alpha^{(i)} f_\beta^{(i)} \tag{7}$$

to the unrelaxed lattice; here $\mathbf{r}^{(i)}$ and $\mathbf{f}^{(i)}$ are the position of, and the force acting on particle i inside the chosen volume, and α, β = x,y,z. As the lattice is unrelaxed, the

total force acting on the volume is not zero, and a straightforward use of formula (7) leads to values which are not independent, as they should be, of the choice of the origin of the coordinates.
The computed field may thus become non symmetric even around a single hydrogen impurity, which is the source of the stress (but not the origin of the coordinates); as shown in fig. 2. To avoid such an unphysical asymmetry, formula (7) has been used by re-defining for each microscopic volume a new origin, located on the atom positioned at the (symmetrical) centre of that volume. The stress tensor defined in this way is, indeed, symmetric around the source of the stress. Since the crystal we are studying has a fcc structure , the palladium atoms are situated also at the centre of its facets, besides at the vertices of each cube of the grid. Corresponding to each of these points we visualized local stresses that are caused from the microscopical interactions with a hydrogen single atom placed at the centre of the crystal. A first interesting information about these data, comes from the visualization of the Miller planes [15]. Such planes {100} {101} {111}, have particular symmetries and they are generally used for representing microscopical dynamics by means of scalar fields. Particularly we can see the visualization of the plane $< 111 >$ in fig. 3. The picture on this plane passing through the impurity indicates that there is a particular zone where the stresses rapidly vary.
The image of figure 4 indicates that the phenomenon can be better understood by means of the glyph tensors visualization. In this image both the scalar field and the tensor field are displayed. In the shaded image the color modifications represent the scalar variable modifications. In this case the scalar variable has been mapped to the shear stress component τ_{xy}.
The bigger glyph is located at the point where there is the impurity and the field is symmetric around it. The icons around the impurity atom clearly show that the stress tensor field decays very rapidly, and it is negligeable outside a volume of a couple atomic cells. The graphic representation allows, nevertheless, to recognize that major principal stress extends mainly along the close packed direction $< 110 >$ and $< 100 >$. Moreover, the glyph's color gives information about the tension and compression states: blue indicates tension and yellow indicates compression. By means of the use of a red scale we can also easily distinguish that the mapped variable has a high variation in the zone where the stress is high.

4 Conclusions

The research described has been addressed to the use of icons, named glyphs, for the representation of second order tensor fields. To this purpose we developed the procedure *Tensor Glyph* and we included it in the MUDI3 system in order to easily experiment this functionality. In this way we had the possibility both to combine more than one visualization technique in the same image and to enhance the quality of the image by means of image transformation functionalities of MUDI3. So Tensor

Glyph has been tested and MUDI3 system has been extended.
Further developments of our work foresee the realization of continuous techniques for the representation of second order tensor fields, mainly by means of hyperstreamlines surfaces and we are also comparing them with the discrete technique here described. Anyway, we would like to point out that the Molecular Dynamics application we studied, demonstrated that discrete representations by means of tensor glyph are better than continuous ones when an analysis of atomic distances phenomena must be carried out.

Acknowledgements:
We thank the Professor Alexander Tenenbaum from the Physics Department of the University of Rome "La Sapienza" for his availability for discussing about the dynamic molecular problem visualizations that we obtained.

References

[1] Kerlick G. D. : *Moving Iconic Objects In Scientific Visualization*, Proc. Visualization 1990, IEEE Computer Society Press, pp. 124 - 130, 1990.

[2] Messina A. , Moltedo L. , Contento S. , Nicoletti R. : *MUDI3 : User-computer interaction; cognitive properties of icons for Multidimensional Data Analysis*, Proc. of WSCG' 95, V. Skala ed., pp. 197-208, 1995.

[3] Haber R.B. : *Visualization techniques for Engineering Mechanics*, Computing System in Engineering , vol. 1, no. 1, pp. 37-50, 1990.

[4] Ascani F. , Messina A. , Moltedo L. : *MUDI3 : a tool for the interactive visual analysis of multidimensional fields* , Proc. NATO A.R.W.: Software for Parallel Computation, I. Kowalik, L. Grandinetti eds., Nato ASI Series F: Computer and systems sciences, vol. 106, Springer Verlag, pp. 203-215, 1993.

[5] Borisenko A.I. , Taparov I.E. : *Vector and tensor analysis with applications*, Prentice-Hall Inc., Englewood Cliff, New Jersey, 1968.

[6] Durelli A.J. , Phillips E.A. , Tsao C.H. : *Introduction to the theoretical and experimental analysis of stress and strain* , Hill book company Inc., New York, Toronto, London, 1958.

[7] Delmarcelle T. , Hesselink L. : *Visualization of Second-Order Tensor Fields with Hyperstreamline*, IEEE Computer Graphics & Applications, vol. 13, no. 4, pp. 25-33, 1993.

[8] Fung Y.C. : *A first course in continuum*, Prentice-Hall Englewood Cliff, New Jersey, 1977.

[9] Comincioli V. : *Metodi Numerici e Statistici per le Scienze Applicate*, Ambrosiana ed., Milano, 1992.

[10] Gaskin T. : *PEXlib Programming Manual*, O'Reilly & Associates, Inc., United States of America, 1992.

[11] Wagner H., *Hydrogen in Metals*, vol. I, G. Alefeld and V. Volkl eds. Springer Verlag, Heidelberg, 1978.

[12] Ducastelle F.: *Tight-binding Potential*, Computer Simulation in Materials Science, M. Meyer and V. Pontilsis eds., Kluwer Academic Publishers, 1991.

[13] Rosato V. , Guillopé Legrand B. , Philosophical Magazine A 59, pp. 321, (1989).

[14] Landau L.D. , Lifshitz E. M. : *Theory of elasticity*, Pergamon Press, London, New York, 1959.

[15] Kittel C. : *Introduction to Solid State Physics*, John Wiley, New York, London, 1963.